Segmentation of Brain Tumor Boundaries using Pattern Recognition of Magnetic Resonance Spectroscopy

Donald J. Peck[1,3], David O. Hearshen[1], Lisa Scarpace[2], Hamid Soltanian-Zadeh[3], Tom Mikkelsen[2]
[1]Henry Ford Hospital, Radiology, Detroit, MI USA; [2]Henry Ford Hospital, Neurosurgery, Detroit, MI USA; [3]Image Analysis Lab - Henry Ford Hospital, One Ford Place, 2F, Box 82, Detroit, MI ;

Introduction

Brain tumors are highly infiltrative and demonstrate a heterogeneous composition that make definition of tumor borders difficult. MRI has been utilized to differentiate the anatomical and morphological features of tumors, but MRI isn´t specific to the heterogeneous features. MR spectroscopy (MRS) has been used to characterize tumors based on measurement of metabolite concentration and has been suggested to be able to differentiate between normal brain, tumor type and therapy induced changes (1-4). Yet, partial volume effects and other variations in the spectra confound definition of the tumor features and specifically in the boundaries between features. In this work, we employed a linear transformation to segment partial volume effects of known spectral patterns from each voxel in order to determine if boundaries of differing tumor components can be defined.

Methods

T1- and T2-weighted MRI from 10 patients with biopsy confirmed low- and high-grade glioma were acquired at 1.5T (GE, Milwaukee, WI) using 24cm FOV, 256x192, and 3mm interleaved slices. MRS images were acquired using a 4-slice spin echo sequence (TR/TE - 2300/272ms) that included water and octagonal outer volume saturation pulses, 24cm FOV, 32x32 phase encoding and 15mm sections. Images of the peak area for each major spectral metabolite, i.e. choline (Cho), creatine (Cr) and N-acetyl aspartate (NAA), were reconstructed after field homogeneity correction. After MRS, post-Gadolinium (Gd) T1 weighted images were acquired. MRI and peak area images from a representative case are shown in Figure 1.

The linear transformation utilized was the Eigenimage filter (EF) (5). The EF has been shown to maximize the SNR of a desired signal while suppressing interfering signals. It also has the advantage of differentiating signals based on partial volume averaging of signals. The steps used in the analysis were:

1. Region of interest (ROI) are used to define normal tissue (i.e. white matter). Spectrum for normal tissue is shown in Figure 2. The EF is then used to remove the normal tissue pattern from the spectrum from each voxel. The pixel value in the resultant image is proportional to the amount of "abnormal" spectral features within each voxel (see Figure 1 – Initial Segmentation).

2. Using the Initial Segmentation image new ROI are defined for voxels displaying the maximum dissimilarity to normal tissue (i.e. "hot"voxels in this image). The spectral pattern from these abnormal voxels and the normal tissue spectra are then used in the EF to create a second segmentation image. In this step the normal and abnormal tissue spectra, as well as any linear combination of both, are removed from each voxel and the resultant pixel values are proportional to the amount of additional spectral features remaining within each voxel. Again ROI are defined for "hot" voxels and used as additional abnormal spectrum in the EF. This procedure is repeated until the resultant image displays only noise. This allows internal tumor heterogeneity to be defined. Once all abnormal spectrum are defined, each is used in the EF to create a separate image of each spectral feature. In these feature images, the partial volume of the normal and all defined abnormal spectra are separated. In the example case three features were found in the iterative procedure. The resultant feature images are shown in Figure 1 (Features 1, 2, and 3) and the corresponding spectrum from each are shown in Figure 2 (Spectrum 1, 2 and 3, respectively).

Results

The initial segmented image removing the normal tissue spectral pattern from each voxel demonstrated the tumor area clearly in both low- and high-grade studies. This can be clearly seen in the example case in Figure 1 – Initial Segmentation image. The area segmented in this image displays the maximum pixel value in the area seen as the Gd enhancement and spreads out from this central zone to encompass an area larger than the abnormality seen on the T2 weighted fast spin echo (FSE) image. Upon further application of the EF, at least two abnormal zones were segmented for both tumor types. Each zone clearly showed differing spectral characteristics (e.g. variations in the number, height, and area of metabolites present). In the example study, three features were found (see Figure 1). The spectral pattern from the maximum intensity region displayed in the segmented images for each feature are shown in Figure 2. Feature 1 shows no NAA peak, a reduced or minimal creatine peak and a large choline peak. In addition, a lactate/lipid peak is present in this area. In Feature 2 the creatine and NAA peaks are increasing. Finally, in Feature 3 the spectrum begins to appear normal, although NAA is reduced relative to the contralateral spectrum and the aspartate peak is not present.

Discussion

We have shown that the EF can differentiate spectral patterns within a tumor and define a map of these features that can be used to determine a boundary for each. The differences in the spectral patterns segmented are clearly due in part to partial volume effects of several tissues within the voxels. It is the fact that the EF can compensates for partial volume effects that allow these differences in spectra to be defined. The determination if these different regions or spectral characteristics can classify tumor pathology or if they are predictive of tumor infiltration is underway using image directed biopsy.

References

1. Taylor JS, et al., Int. J. Rad. Onc. Biol. Phys., 36, p1251-61, 1996.
2. Preul MC, et al., Can. J. Neurol. Sci., 25, p13-22, 1998.
3. Poptani H, et al., J. Cancer Res. Clin. Oncol., 125, p343-9, 1999.
4. Nelson SJ, et al, NMR Biomed., 12, p123-38, 1999.
5. Peck DJ, et al., Med. Phys., 23, p2035-42, 1996.

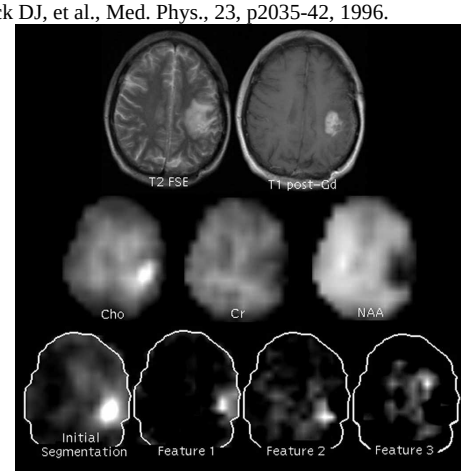

Figure 1

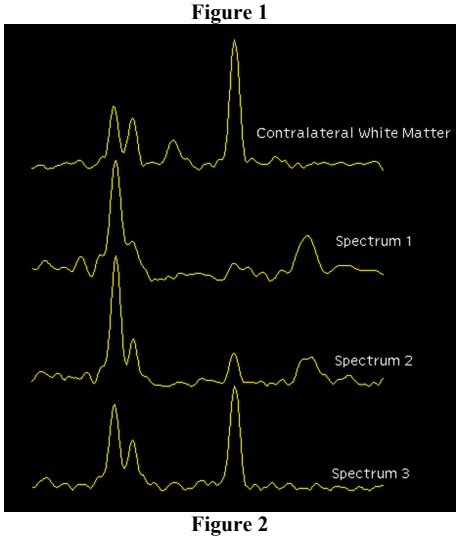

Figure 2